ELSEVIER

Physica D 108 (1997) 147–167

PHYSICA D

Transition fronts and localized structures in bistable reaction–diffusion equations

Bard Ermentrout *, Xinfu Chen [1], Zhixiong Chen

Department of Mathematics, University of Pittsburgh, Pittsburgh, PA 15260, USA

Received 10 June 1996; received in revised form 31 January 1997; accepted 3 February 1997
Communicated by J.D. Meiss

Abstract

Models of chemical reactions that undergo subcritical Hopf bifurcations and have a regime of bistability are shown to exhibit some interesting behavior when diffusively coupled. Waves joining a stable steady state to a periodic wavetrain are constructed for low and high thresholds. For intermediate thresholds, localized oscillatory regions are found. These can interact at a distance and behave like weakly coupled oscillators. These patterns are found in both solvable and realistic models for chemical oscillations.

Keywords: Oscillations; Bistability; Waves

1. Introduction

Reaction–diffusion systems have provided the canonical example of spatio-temporal pattern formation (see [1,3,7] for examples.) The variety of patterns in these systems range from simple oscillations and waves to complex spatio-temporal phenomena [12]. In this paper, we will describe and analyze some phenomena that occur in simple reaction–diffusion models. We will consider systems in which there are two stable states: a stable fixed point and a stable limit cycle. Such a situation is common in systems with excitable dynamics. As some parameter changes the system goes through a subcritical Hopf bifurcation with a parameter interval where there is a stable rest state and a stable large-amplitude periodic orbit. An unstable periodic orbit acts as the separatrix between the two states. In a recent paper, Kobayashi et al. [9] study the dynamics of this situation and find a variety of wavefronts and other solutions. By varying the diffusion coefficient of one of the species, they exhibit transitions from traveling fronts joining the fixed point to a periodic orbit to spatially localized oscillatory structures and ultimately to disordered structures. They also study some of the behavior in two space dimensions. In a related paper Thual and Fauve [16] show the existence of localized oscillatory structures in a variant of the complex Ginzberg–Landau equations.

* Corresponding author. Supported in part by NSF DMS-96-26728.

[1] Supported in part by NSF DMS-96-22872.

PII S0167-2789(97)00033-X

We will build on these results; in particular, we study the transition from waves to isolated patches of oscillatory behavior as a function of the threshold. We also attempt to understand the traveling waves that are left in the wake of the fronts.

Fronts joining differing states are well known in reaction–diffusion systems, particularly in the scalar case. The Fisher equation

$$u_t = u(1-u) + u_{xx}$$

provides the standard example. Here there are infinitely many fronts that join the *unstable* state 0 to the stable state 1. The particular front chosen and the velocity of the front depends intimately on the initial data [17]. An analogous phenomena has been described extensively by Sherratt [13–15] for fronts joining an unstable rest state to an oscillatory solution. Sherratt studies a simple $\lambda - \omega$ system:

$$z_t = zf(z\bar{z}) + z_{xx},$$

where $f(r^2) = 1 - r^2 + \mathrm{i}\omega(r^2)$. In absence of diffusion, there is a stable periodic solution ($z = \mathrm{e}^{\mathrm{i}\omega(1)t}$) and an unstable fixed point ($z = 0$). Sherratt shows with a combination of formal estimates and numerical studies that there are infinitely many wavefronts joining the unstable rest state to one of many different plane wave solutions. He shows that, like the Fisher equation, the velocity and form of the traveling waves are dependent on the initial data.

Wavefronts between systems with *two stable* states behave quite differently. For example, in the bistable reaction–diffusion system

$$u_t = u(u-a)(1-u) + u_{xx},$$

there is a unique traveling wave that joins the *stable* state $u = 0$ to the other stable state $u = 1$. All sufficiently large initial data evolve into wavefronts with this velocity [4]. Klassen and Troy [8] proved an analogous result for system of two coupled reaction–diffusion equations in which there were two stable fixed points but diffusion on only one variable. In general, however, the behavior of systems with two stable fixed points can be quite complicated. Haim et al. [5] and Pearson [12] have shown the existence (through simulations and experiments) of complicated spatio-temporal behavior when a bistable system is coupled with diffusion. For example, Haim et al. have found "breathing spots" in a two-dimensional flow reactor model. Pearson observes spots that split into new spots and a variety other complicated spatio-temporal patterns that have been subsequently experimentally verified.

Here we will explore the behavior of systems of reaction–diffusion equations which admit a stable periodic orbit and a stable fixed point separated by an unstable periodic orbit. As mentioned above, Kobayashi et al. [9] consider this situation and treat the diffusion of one of the variables as a parameter. They numerically study behavior of a simple nonlinear reaction–diffusion equation on the line and in a two-dimensional square domain. Our goal is to study the transition waves and the selection mechanism for the velocity of the front as well as the asymptotic behavior of the medium after the front has passed. In particular, we are interested in the wavelength of the resultant plane waves. Finally, we look at the localized patterns described by Kobayashi et al. [9] and by Thual and Fauve [16].

In Section 2, we numerically examine a simplified version of the Field–Noyes equations and show the transition waves. We turn to a variation of the complex Ginzberg–Landau equations that arises near a subcritical Hopf bifurcation. We are able to explicitly compute a unique wavefront joining the two stable states. We show that this exists only for some ranges of parameters. In Section 3, we show that localized oscillations occur for parameters outside the range in which front solutions exist. We explore their interactions in one- and two-dimensions and show how they behave like discrete weakly coupled oscillators.

2. Traveling waves

We begin this section with some numerical examples of a chemical system that has "realistic" kinetics. We choose a simplified model of the Belousov–Zhabotinskii model which is descibed in [11]. We arrange the parameters for this model so that there is a coexistent stable fixed point and a limit cycle which surrounds it. The model equations are:

$$\frac{dy}{dt} = u - z \equiv F(y, z), \tag{2.1}$$

$$\frac{dz}{dt} = (2fz - y(u + p))/\delta \equiv G(y, z), \tag{2.2}$$

$$u = \tfrac{1}{2}\left(1 - y + \sqrt{(1 - y)^2 + 4qy}\right),$$

where $f = 0.3$, $p = 0.001$ and δ is varied. In addition to the stable fixed point and limit cycle is an unstable limit cycle which provides the separatrix between the two stable states. This type of picture arises anytime there is a subcritical Hopf bifurcation branch which turns around. The bifurcation diagram for this system is shown in Fig. 1(A) using δ as a parameter. Fig. 1(B) and (C) show the phase plane for two different values of δ in the region where the system is bistable. The bistability occurs for all values of δ between $\delta = \delta_H = 0.191$, the Hopf bifurcation point and $\delta = \delta_L = 0.269$, the limit point of the branch of periodic solutions. For $\delta > \delta_H$ there is a unique stable fixed point and for $0 < \delta < \delta_L$ there is a unique stable limit cycle. We use these kinetics in a reaction–diffusion system:

$$\frac{\partial y}{\partial t} = D_y \frac{\partial^2 y}{\partial x^2} + F(y, z), \qquad \frac{\partial z}{\partial t} = D_z \frac{\partial^2 z}{\partial x^2} + G(y, z). \tag{2.3}$$

Since the model system is intrinsically bistable, we ask what happens if a small patch of the medium is excited from rest into the oscillatory regime. The result of such a simulation is shown in Fig. 2(A) for $\delta = 0.195$ (corresponding to the phase plane in Fig. 1(B).) The result shows a wave that propagates across the medium with constant velocity and which switches the system from a stable fixed point to a stable periodic wave. The trailing wavetrain appears to have a unique wavelength. The velocity and wavelength of the wave are *independent of the initial condition.*

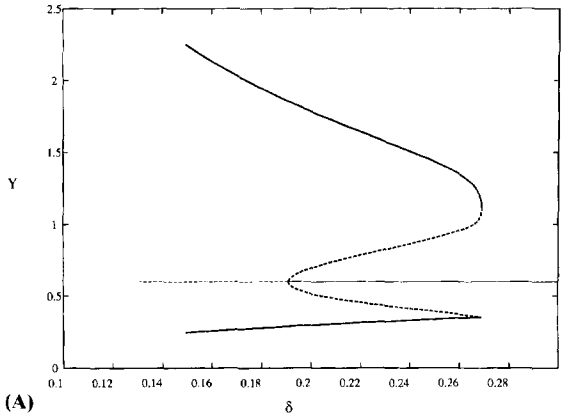

Fig. 1. Behavior of the chemical system. (A) Bifurcation diagram showing the coexistence of stable periodic orbits (thick solid lines) and stable fixed points (thin solid lines) for a range of δ. (B), (C) Phase planes for $\delta = 0.195$ and $\delta = 0.202$. The unstable periodic orbit (shown as the small solid circle) serves as the separatrix between the stable periodic orbit and the fixed point.

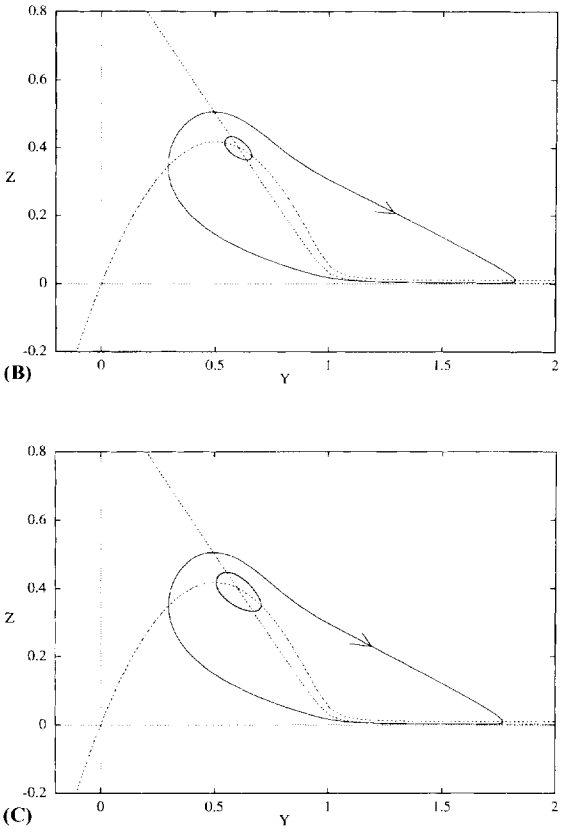

Fig. 1. Continued

This fact distinguishes these switching waves from those studied by Sherratt [13,14] for which there were infinitely many possible velocities and corresponding wavelengths. The kinetics Sherratt uses have an *unstable* fixed point and a stable limit cycle whereas in our system both the fixed point and the limit cycle are asymptotically stable. In the simulation shown in Fig. 2(A) we have chosen δ near the point of the Hopf bifurcation. Thus, in a sense, the "threshold" for excitation to the limit cycle is small. If we choose δ close to the limit point δ_L, then it is possible to observe a wave that switches the medium from the oscillatory state to the rest state. This wave is not simply the reverse of the other front; the medium ahead of the front oscillates *synchronously* rather than with some finite wavelength.

If the medium is started at the stable fixed point and the "threshold" is low, then a sufficient large local perturbation into the domain of attraction of the limit cycle grows and spreads at a constant velocity across the medium. In its wake, it leaves a periodic wavetrain which is *not* generally synchronous. Instead, there is a clear phase-lag correponding

Fig. 2. Example wavefronts joining a periodic solution to a stable fixed point. In all figures, space is horizontal and time increases vertically downward. (A) A typical front for the chemical model with parameters as in Fig. 1(B). Domain length is 20 and total time is 200. The value of $y(x,t)$ is coded in gray scale; black corresponds to 1.8 and white to 0.1. Parameters are $f = 0.3$, $q = 0.001$, $\delta = 0.195$, $D_y = D_z = 0.2$; kinetics are as in Fig. 1(B). (B) A wavefront for a simple nerve model showing wavetrains with very short wavelength compared to (A). (C) Same model as in (B) with different threshold showing waves that join the synchronous solution to the fixed point. Both (B), (C) show the voltage as a function of time.

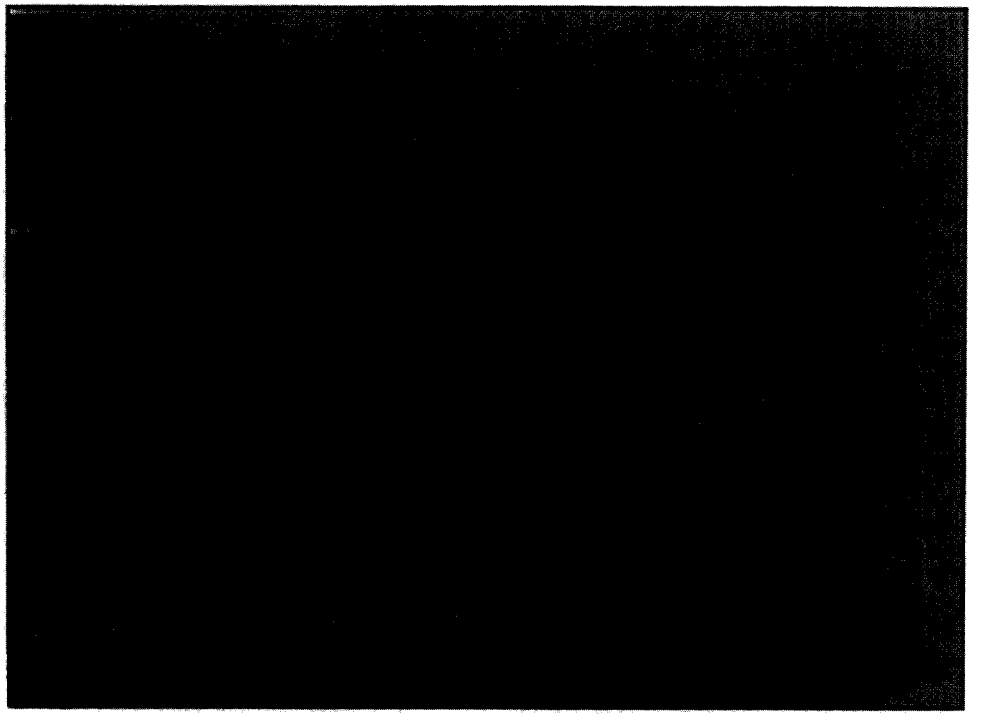

(A)

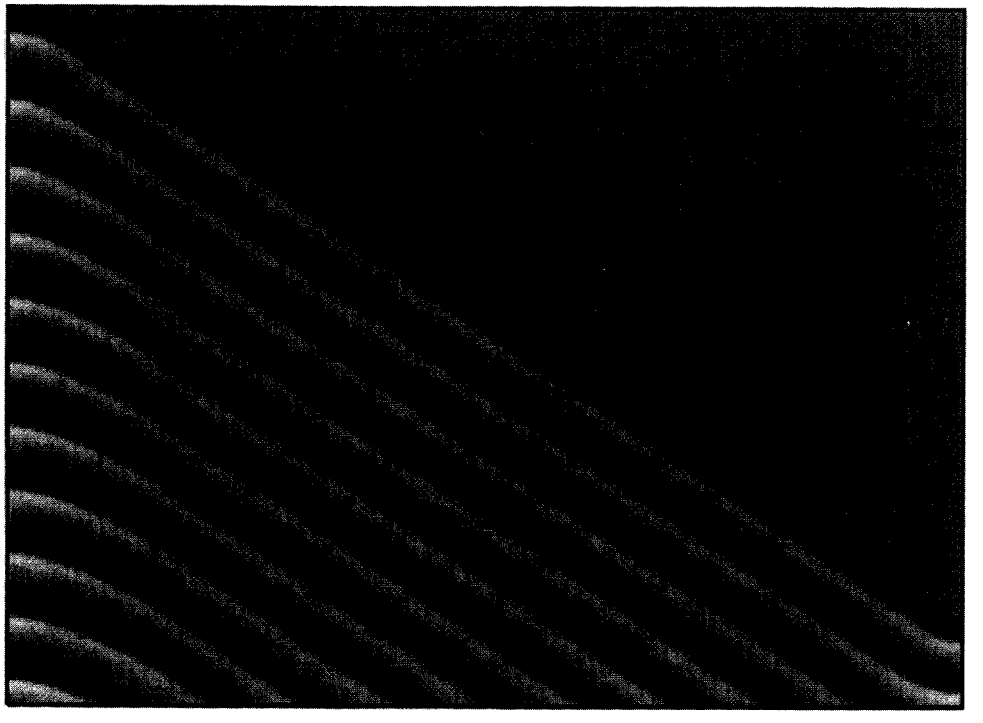

(B)

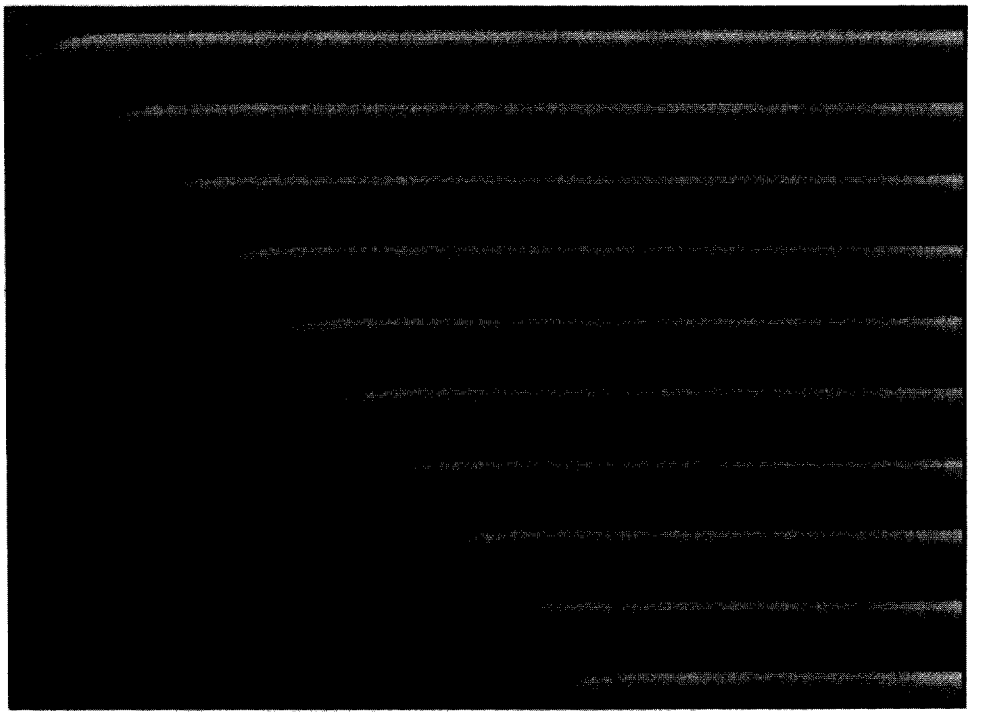

Fig. 2. Continued

to a particular traveling wavetrain. The front velocity and the wavelength are unique and independent of the initial data. On the other hand, suppose the medium is started from a uniformly oscillating state and the "threshold" is high. A local perturbation to the fixed point can then grow and propagate across the medium. Thus, unlike the former wavefront which joins the fixed point to a wavetrain with a distinct wavelength, the wave described here joins the *synchronous oscillation* to the fixed point. Unlike the case of a reaction–diffusion equation with two stable fixed points, here, the switching front is qualitatively different depending on whether the fixed point or the oscillation "dominates".

Fig. 2(B) and (C) shows another simulation; this one is a simplified nerve model. Fig. 2(B) shows the wave that switches the medium from rest to an oscillatory state. Here the bifurcation parameter is near the Hopf bifurcation so that the domain of attraction of the fixed point is small. Note that the wavelength of the resultant wave train is much shorter than that of the chemical example. As in the chemical example, the system is bistable with a single stable fixed point separated from a stable oscillation by an unstable periodic orbit. Fig. 2(C) shows a wave that switches the medium from the synchronous oscillation to the rest state. In this case, the bifurcation parameter is adjusted to be near the limit point of the large amplitude periodic; the domain of attraction of the stable limit cycle is very small. Notice that the wave connects the rest state to the *synchronous* state.

One observation is that the front velocity does not have to match the phase velocity of the traveling waves. That this is not true is clear from Fig. 2(A) and (C) where the phase velocity is very large (the trailing oscillations are nearly synchronous which correspond to infinite phase velocity).

The simulations suggest that there is a unique wavelength selected for fronts that switch the medium from rest to an oscillatory state. We turn our attention to showing that this is the case for a simplified model.

2.1. An exactly solvable model

We consider a simplified reaction–diffusion system that has many of the properties of the above two examples. In addition, we can explicitly determine the unique velocity of the switching front and the wavelength of the trailing wave train. The system is a $\lambda - \omega$ system modified so that there are both a stable fixed point and a stable limit cycle:

$$\frac{\partial u}{\partial t} = \lambda(u^2 + v^2)u - \omega(u^2 + v^2)v + D\frac{\partial^2 u}{\partial x^2}, \tag{2.4}$$

$$\frac{\partial v}{\partial t} = \lambda(u^2 + v^2)v + \omega(u^2 + v^2)u + D\frac{\partial^2 v}{\partial x^2}, \tag{2.5}$$

where

$$\lambda(r^2) = (1 - r^2)(r^2 - a^2), \qquad \omega(r^2) = \omega_0 + qr^2.$$

The reaction kinetics for this system arise near a Hopf bifurcation when the branch is nearly vertical. (In the usual Hopf normal form, the kinetics is strictly cubic; the fifth-order term is needed when the cubic term is near zero. This can be considered the normal form for a subcritical Hopf bifurcation where the branch turns around.) (We remark that Thual and Fauve [16] have studied a system similar to this which they note arises from a fluid flow problem. They were mainly interested in the localized spatial structures which we discuss in the next section.) We have set the diffusion coefficient to $D = 1$ with no loss of generality since space can always be rescaled.

In absence of diffusion, there are two stable states: $(u_0, v_0) = (0, 0)$ and $(u_s(t), v_s(t)) = (\cos \Omega t, \sin \Omega t)$ where $\Omega = \omega_0 + q$. In addition, there is an unstable periodic solution $(u_u(t), v_u(t)) = (a \cos \Omega t, a \sin \Omega t)$, where $\Omega = \omega_0 + qa^2$. Thus, the spatially homogeneous sytem is bistable with a stable rest state and a stable oscillatory solution.

Scalar diffusive coupling has no effect on the stability of the rest state, nor on the stability of the homogeneous oscillation, thus, the homogeneous oscillation and the fixed point are stable as solutions to the partial differential equation.

The parameter q is important; it arises generically in perturbation calculations, and it is responsible for the dispersive property of the wavetrains. We first discuss the plane wave solutions. For each $k \in [0, \frac{1}{2}(1 - a^2))$ there are two plane wave solutions to (2.4) of the form

$$u(x, t) + iv(x, t) = R^{\pm} e^{ikx} e^{i\Omega^{\pm} t} \equiv Z^{\pm}(k; x, t)$$

with $0 < R^- \leq R^+$, and

$$R^{\pm} = \sqrt{\frac{(1 + a^2) \pm \sqrt{(1 - a^2)^2 - 4k^2}}{2}}$$

and

$$\Omega^{\pm} = \omega_0 + q\left(R^{\pm}\right)^2 = \omega_0 + \tfrac{1}{2}q[(1 + a^2)^2 \pm \sqrt{(1 - a^2) - 4k^2}].$$

Note that for $k = 0$ we recover the two homogeneous oscillations; the larger amplitude oscillation R^+ is stable and the smaller R^- is unstable. Thus, we will only consider the positive branch of these solutions. The velocity of the waves is Ω^+/k. Note that if $q = 0$, the frequency of the waves is independent of the amplitude R and wave number k. Of the family of plane waves connected to R^+ a band of them near $k = 0$ will be asymptotically stable [10]. This suggests that there might be a variety of fronts connecting the stable rest state $(u, v) = (0, 0)$ to any one of

the plane waves. As we will see shortly, this is not the case; rather there appears to be a unique plane wave selected and a unique propagation velocity for the front.

Before turning to the analysis of the fronts, we show some numerical simulations of (2.4) and (2.5) for different values of q. When $q = 0$ the wavefront joins the stable rest state to the homogeneous oscillation. For nonzero values of q the asymptotic state is a traveling wave with a nonzero wave number; if $q > 0$, the wavetrains move downward as in Fig. 3(A) while if $q < 0$, they move in the opposite direction as in Fig. 3(B). Note that the front velocity is the same for both waves. This picture should be contrasted to those in [13,14] where for any given set of parameters, there are many possible connection fronts. (Sherratt uses a different functional form for $\omega(r)$ namely, $\omega(r) = ar^p$. Only for $p = 0, 2, 4, \ldots$ does this form arise in the context of normal forms near a Hopf bifurcation.)

We now state and prove the main result of this section.

Proposition 1. Assume that $\frac{1}{2}\sqrt{3}q \in (0, \frac{1}{2}(1-a^2))$ and for each $k \in [0, \frac{1}{2}(1-a^2))$ let $Z^{\mp}(k; x, t)$ be the plane wave solution constructed above. Then for $k = k^* \equiv \frac{1}{2}\sqrt{3}q$ there exists a traveling wave connecting 0 and $Z^{\pm}(k^*, x, t)$. That is there exists a real-valued function, $h^{\pm}(\xi)$ and a real-valued $c^{\pm}$ such that

$$u + \mathrm{i}v \equiv h^{\pm}(x - c^{\pm}t)Z^{\pm}(k^*; x, t) \tag{2.6}$$

is a solution to (2.4) and (2.5) where $h^{\pm}$ satisfies

$$\lim_{\xi \to -\infty} h^{\mp}(\xi) = 0, \qquad \lim_{\xi \to +\infty} h^{\mp}(\xi) = 1.$$

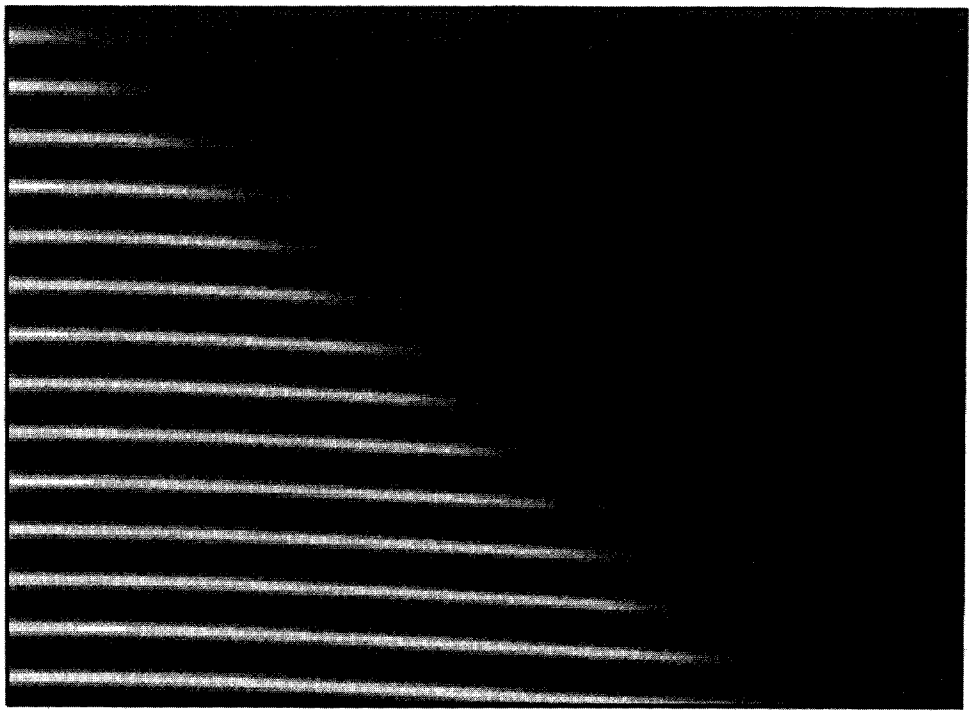

Fig. 3. Simulations of the $\lambda - \omega$ system for $a = 0.25$ on a domain of length 40. (A) $q = 0.25$, (B) $q = -0.2$. Note that in the first panel, the wavetrain velocity is the same sign as the front velocity but in the second panel the train velocity is negative. Total time of simulation is 80.

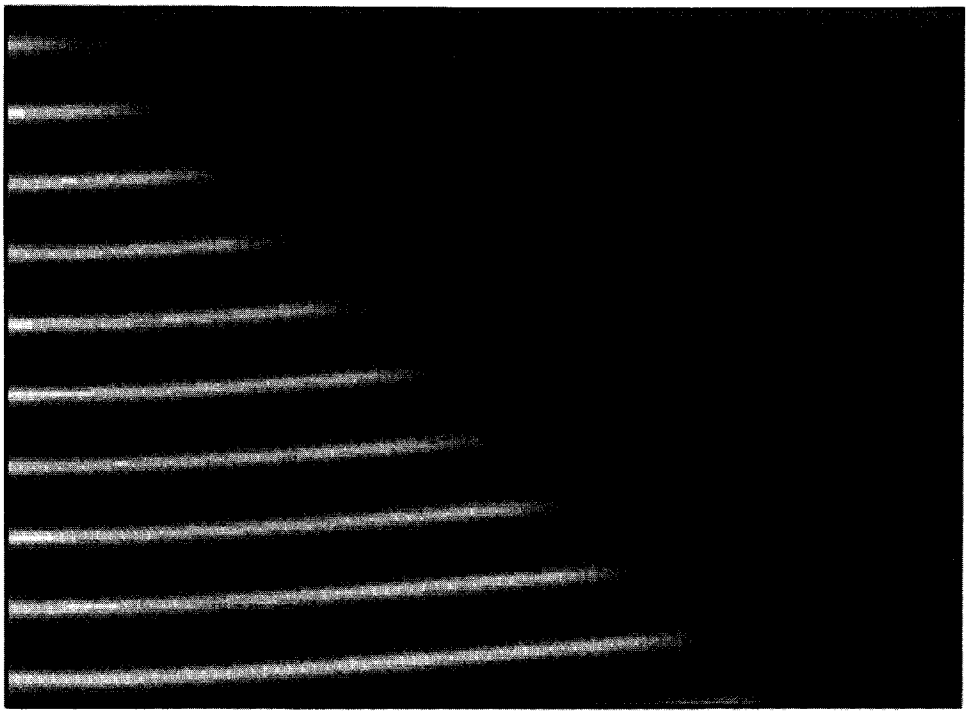

Fig. 3. Continued

In addition, $c^{\pm}$ has the following signs:

$$c^- > 0 \quad \text{for all } a \in (0,1) \text{ and } q \in \left(0, \frac{1-a^2}{\sqrt{3}}\right),$$

$$c^+ > 0 \quad \text{if } a > \frac{1}{\sqrt{3}} \text{ or } a \le \frac{1}{\sqrt{3}} \text{ and } q > \frac{1}{\sqrt{3}}\sqrt{(1-a^2)^2 - (1+a^2)^2/4},$$

$$c^+ = 0 \quad \text{if } a \le \frac{1}{\sqrt{3}} \text{ and } q = \frac{1}{\sqrt{3}}\sqrt{(1-a^2)^2 - (1+a^2)^2/4},$$

$$c^+ < 0 \quad \text{if } a \le \frac{1}{\sqrt{3}} \text{ and } 0 \le q < \frac{1}{\sqrt{3}}\sqrt{(1-a^2)^2 - (1+a^2)^2/4}.$$

Remark 1.

(1) The case in which $q < 0$ is obtained in the same manner.

(2) Negative velocities correspond to fronts in which the oscillatory solution "takes over" while for positive velocities, the fixed point "takes over". Not surprisingly, the unstable periodic orbit is always dominated by the stable fixed point; c^- is always positive.

(3) We expect the fronts that tend to Z^- are unstable since they corrspond to a family of unstable plane waves. Our numerics indicate that those that correspond to stable plane waves are also stable when the velocity is negative. That is, the fronts constructed here agree with numerical simulations in which the medium switches from *rest to oscillation.*

(4) $a > 1/\sqrt{3}$ iff $(1-a^2)^2 < \frac{1}{4}(1+a^2)^2$.

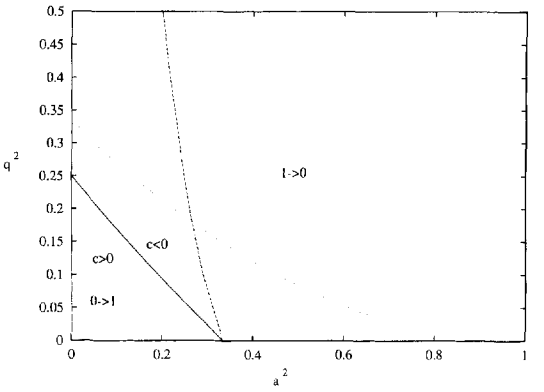

Fig. 4. Diagram showing the ranges of the parameters a^2 and q^2 for which there are fronts. Region labeled 0->1 is where there are fronts in which the rest state is overtaken by the periodic wavetrain according to Proposition 1. In this region, the velocity is negative. The dotted lines delineate the region of existence of the waves describe in Proposition 1. The region labeled 1->0, numerically determined, is where there are fronts in which the rest state overtakes the synchronous oscillation.

(5) Fig. 4 shows a plot of the range of existence and where the waves have negative velocity.
(6) The proposition suggests that the selected wave number is $k = \frac{1}{2}\sqrt{3}q$. In particular, when $q = 0$, the wavefront joins the rest state to the synchronous oscillation.
(7) Plane waves exist for any q but the fronts do not appear to exist for $q > (1 - a^2)/\sqrt{3}$.

Proof. We rewrite the system in terms of new variables, r, θ where $u + iv = re^{i\theta}$. Eq. (2.4) becomes

$$r_t = r(1 - r^2)(r^2 - a^2) + r_{xx} - r\theta_x^2, \tag{2.7}$$

$$\theta_t = \omega_0 + qr^2 + \frac{2r_x\theta_x}{r} + \theta_{xx}, \tag{2.8}$$

where the subscripts mean derivatives as usual. When $q = 0$ we take $\theta = \omega_0 t$ and are left with the equation for r:

$$r_t = r(1 - r^2)(r^2 - a^2) + r_{xx}.$$

The results of Fife and McLeod [4] imply that there is a unique traveling wave from $r = 0$ to $r = a$ and another one joining $r = 0$ and $r = 1$. The latter is the front joining the fixed point to the synchronous large-amplitude periodic solution and the former joins the fixed point to the unstable periodic orbit. Thus, the case $q = 0$ follows from the behavior of the scalar bistable system. We now suppose that $q > 0$. Assume that the solutions have the form

$$\theta = k(x - ct) + (\Omega + \omega_0)t, \qquad r = H(x - ct).$$

(Note that the phase gradient θ_x is constant. There is no a priori reason to expect this for general reaction–diffusion models. However, in $\lambda - \omega$ systems periodic plane waves always have a constant phase gradient.) We have to find $H(\xi)$ such that *both* of the following differential equations are satisfied:

$$H'' = k^2H - cH' - H(1 - H^2)(H^2 - a^2), \tag{2.9}$$

$$H' = \frac{H}{2k}[\Omega - qH^2 - ck]. \tag{2.10}$$

Let $\mu = (\Omega - ck)/q$ and let H be the solution to (2.10), i.e.

$$H' = \frac{qH}{2k}(\mu - H^2), \quad H(-\infty) = 0, \quad H(+\infty) = \sqrt{\mu}, \quad H' > 0.$$

Then we can calculate

$$H'' = \frac{q^2}{4k^2}H(\mu - H^2)(\mu - 3H^2) = \frac{3q^2}{4k^2}H\left[H^4 - \frac{4}{3}\mu H^2 + \frac{\mu^2}{3}\right],$$
$$k^2 H - cH' - H(1 - H^2)(H^2 - a^2) = H\left[H^4 - \left(1 + a^2 + \frac{qc}{2k}\right)H^2 + k^2 + a^2 + \frac{qc}{2k}\mu\right].$$

Hence, for (2.9) to hold, we need only match the coefficients of the powers of H:

$$\frac{3q^2}{4k^2} = 1, \qquad \frac{4}{3}\mu = 1 + a^2 + \frac{qc}{2k}, \qquad \frac{\mu^2}{3} = k^2 + a^2 + \frac{qc}{2k}.$$

We can rewrite these as

$$k^2 = \frac{3}{4}q^2, \qquad 0 = \mu^2 - (1 + a^2)\mu + k^2 + a^2, \qquad c = \frac{2k}{q}\left[\frac{4}{3}\mu - (1 + a^2)\right]$$

with Ω determined by the relation

$$\Omega = ck + \mu q.$$

Taking $k = \frac{1}{2}\sqrt{3}q$ (if $k = -\frac{1}{2}\sqrt{3}q$ then reverse the sign of c) we have

$$k = \frac{\sqrt{3}}{2}q, \qquad \mu = \tfrac{1}{2}\left(1 + a^2 \pm \sqrt{(1 - a^2)^2 - 3q^2}\right) = \left(R^{\pm}\right)^2,$$
$$c = \left((1 + a^2) \mp 2\sqrt{(1 - a^2)^2 - 3q^2}\right)\Big/\sqrt{3}, \qquad \Omega = \mu q + ck.$$

Thus,

$$u + \mathrm{i}v = H(x - ct)\mathrm{e}^{\mathrm{i}k(x-ct)}\mathrm{e}^{\mathrm{i}(\Omega+\omega_0)t} = H(x - ct)Z^{\pm}(k; x, t)/R^{\pm}.$$

Since

$$c^{\pm} = \left[(1 + a^2) \mp 2\sqrt{(1 - a^2)^2 - 3q^2}\right]\Big/\sqrt{3},$$

we see that $c^- > 0$ and c^+ can be positive, zero, or negative. □

Numerical simulations of the model agree with the calculations of Proposition 1 as long as the waves represent a switch from rest to the oscillatory state. Notice that if $q > 0$ is fixed, then for a close to 1, no waves of this form exist. However, numerical simulations show that there are in fact wavefronts but that they switch the system from a *synchronized* oscillatory state to the stable rest state. In this case, the asymptotic wave number is 0. We also find that the phase gradient $\phi \equiv \theta_x$ is not constant for these waves. Instead there seems to be a family of traveling waves that are not of the simple form described above. Instead, we conjecture that for a large (near $a = 1$), the waves have the form

$$u + \mathrm{i}v = \rho(x - ct)\mathrm{e}^{\mathrm{i}\Omega t + \int_0^{x-ct}\phi(\eta)\,\mathrm{d}\eta} \tag{2.11}$$

where, $\Omega = \omega_0 + q$,

$$\lim_{\xi\to-\infty}(\rho(\xi), \phi(\xi)) = (0, 0) \quad \text{and} \quad \lim_{\xi\to+\infty}(\rho(\xi), \phi(\xi)) = (1, 0).$$

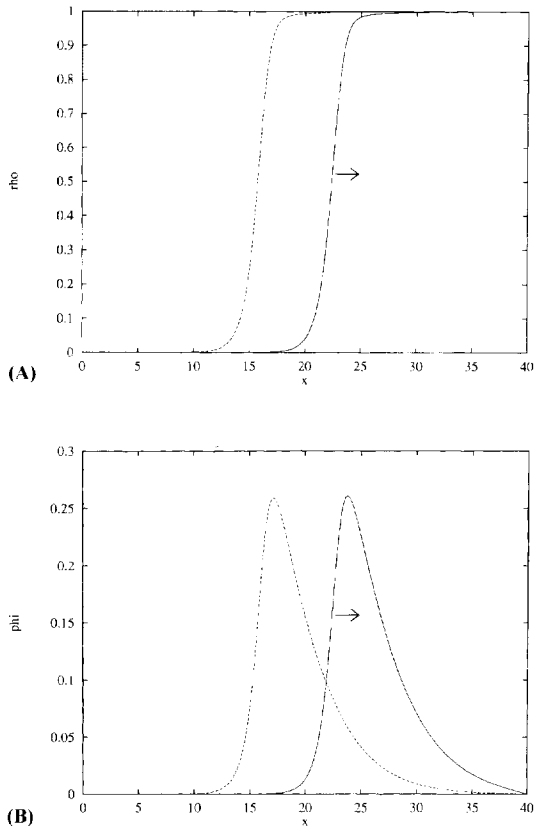

Fig. 5. The behavior of wavefronts which take the $\lambda - \omega$ system from the synchronous oscillation to the stable rest state. (A) Profile of the amplitude $R(x, t)$ as a function of space at two different times. (B) Profile of the phase gradient $\phi(x, t)$ as a function of space at two different times (arrows show direction of motion).

(Note that by multiplying (2.8) by r to eliminate r in the denominator, we see that $r = 0$ is a fixed point and so (2.11) could be a form for the solution.) Fig. 5 shows a simulation for $q = 0.2$ and $a = 0.6$. The first panel shows the spatial profile of the amplitude ρ at two different times. The second shows the phase gradient ϕ at the same two times. Note that in advance and behind the wave ϕ vanishes indicating that the oscillation in front of the wave is synchronous.

The calculations of Proposition 1 are relevant only for (a, q) such that $c^+(a, q) < 0$. Fig. 4 shows a plot of q^2 versus a^2 delineating the regions where the velocity is negative and the solutions of Proposition 1 exist. It is clear that if $q > \frac{1}{2}$ then there are no switching waves from rest to the oscillatory state. Similarly, if the threshold a is larger than $1/\sqrt{3}$ then there are also no switching waves of the form in Proposition 1. Numerical simulations confirm that there are no other stable waves which switch the rest state to the oscillatory state. The figure also shows a numerically computed curve showing the range of (a, q) where there are waves that switch the medium from the synchronous oscillatory state to the rest state. These are not of the form in Proposition 1 but instead of the form described in the previous paragraph e.g. Eq. (2.11). Thus, a combination of numerical simulations (for a large) and the results of Proposition 1, (for a small) lead us to conclude that the (a, q) parameter space is broken into three regimes: (i) for (a, q) small, there are fronts switching the system from rest to a periodic wavetrain; (ii) for a large, there are fronts switching the system from a synchronous oscillation to the rest state; (iii) for (a, q) between these two regimes, we will see below that localized oscillatory patches occur.

3. Local spatial oscillators

3.1. Local oscillations "between the fronts"

In Section 2, we showed that there were traveling fronts for the bistable $\lambda - \omega$ model as long as (a, q) was in one of two regions. Suppose that (a, q) does not lie in the regions where there are wavefronts. Then numerical solutions show that sufficiently large localized perturbations from the synchronous oscillatory state or the rest state evolve into a spatially localized oscillatory state surrounded by medium near rest. Fig. 6 illustrates a localized region obtained when $a = 0.25$ and $q = 0.5$. (We plot the amplitude so that the actual oscillatory activity is not evident in the figure.) We have started the medium at rest and perturbed a region slightly to the left of center (in order to avoid any consequences of special symmetry). The active region begins to spread but then stops and leaves a localized spatial oscillation. The localized disturbance moves to the left boundary where it persists. In larger domains, the attraction to the boundary can be almost imperceptible and for all intents and purposes, the local oscillation remains at the spatial position close to the initial disturbance. In an infinite domain, there are no boundary effects and the oscillation will remain stationary.

There have been several reports of localized oscillating regions in active media (see the work of Mimura, etc.) often called "breathers". The mechanism for breathers is quite different from the present case. Breathers arise in systems with excitable dynamics (a unique globally attracting fixed point for the reaction kinetics with a threshold and amplification of sufficiently large stimuli before returning to rest) and "lateral inhibition". The latter requires

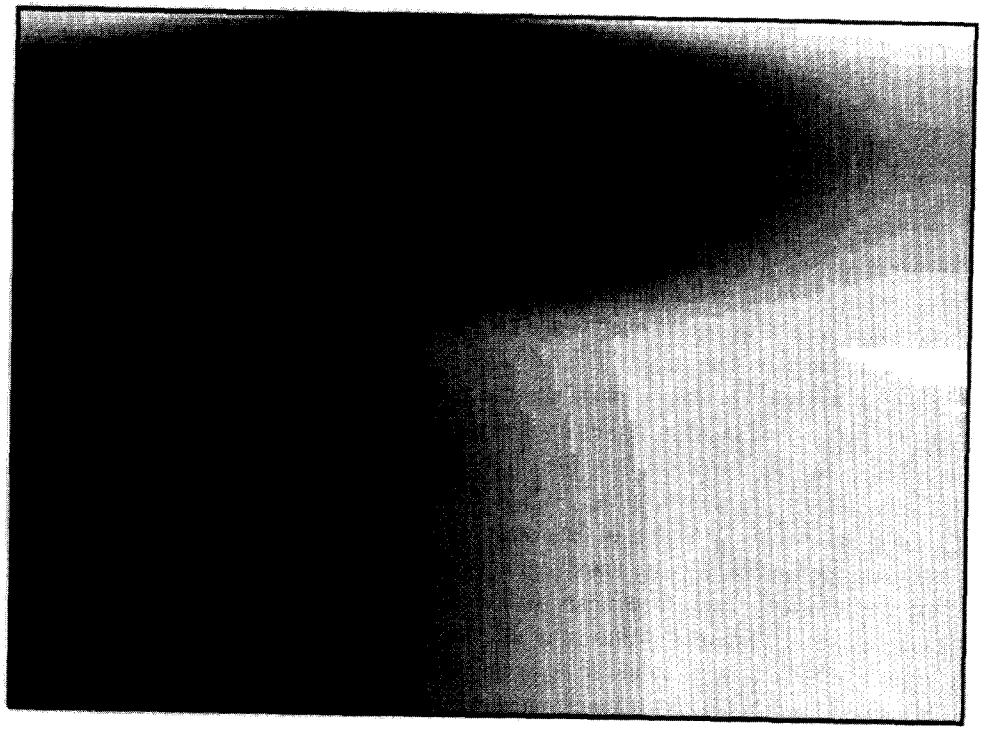

Fig. 6. Evolution of the amplitude $r = \sqrt{u^2 + v^2}$ from an initial disturbance centered at $x = 8$ in a domain of length 20 for the $\lambda - \omega$ system with $a = 0.25$, $q = 0.5$. Dark region corresponds to higher amplitude and oscillatory behavior while light region is the rest state. Total simulation time is 200.

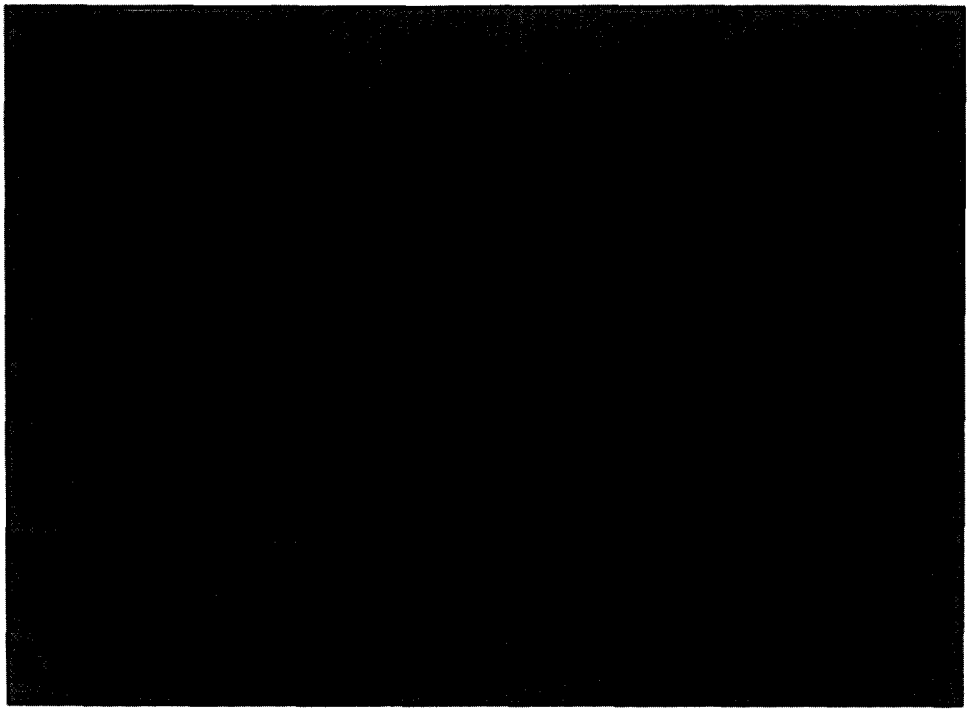

Fig. 7. Evolution of a localized spatial oscillation in the chemical model. Initial disturbance at $x = 3$ in a medium of length 20. Total time of simulation is 400. Parameters and plot are as in Fig. 2(A) except that $\delta = 0.202$ corresponding to the kinetics in Fig. 1(C).

that the diffusion constants of the two species be quite different. The result of these assumptions is often a spatially localized pulse. As the time constant of one of the species changes the local pulse loses stability via a Hopf bifurcation and begins to oscillate. The oscillations remain localized in space. The localized oscillation observed in Fig. 6 arises in a medium which is bistable with a coexistent stable limit cycle and a stable fixed point. Furthermore, there is little difference in the magnitude of the diffusion coefficients. Kobayashi et al. [9] found such pulses in their numerical exploration of a related bistable system as they varied the diffusion of the "recovery" variable.

Such pulses exist in the chemical model (2.1) and (2.2) as well. The parameter δ plays the role of a in that as δ varies the domain of attraction of the rest state and the stable limit cycle also vary. As δ increases, the domain of attraction for the stable fixed point increases until at the value $\delta > \delta_L$ the entire first quadrant is attracted to the stable fixed point. Thus, we increase δ from the value $\delta = 0.195$ which produced Fig. 2(A) to $\delta = 0.202$. The phase plane for this value of δ is shown in Fig. 1(C). A simulation of (2.3) is depicted in Fig. 7. The medium is initially at rest and a perturbation to the left of the center is made. A rather large region begins to oscillate but this shrinks eventually settling to a spatially localized region of oscillatory activity. As in the $\lambda - \omega$ model, we believe that this slowly moves toward the nearest boundary. However, as seen in Fig. 7, the movement is imperceptible. (We continued this simulation for 10 times the amount of time shown in the figure and observed very little movement.)

This behavior persists for a range of values of δ. As the threshold increases, that is, as δ increases, this localized region shrinks to a point. Then there exists a wavefront which switches the medium from the synchronous oscillatory state to the fixed point, just like the $\lambda - \omega$ model.

The bistable systems (2.3) and (2.4)–(2.5) appear to have ranges of parameters in which there are stable spatially localized oscillations. Numerical simulations of (2.3) indicate that there are three ranges for the parameter δ: (i) for

$\delta \in (\delta_H, \delta_1)$ there is a wavefront which switches the medium from rest to oscillation; (ii) for $\delta \in (\delta_1, \delta_2)$ there is a localized oscillation; and (iii) for $\delta \in (\delta_2, \delta_L)$ there is a front switching the medium from oscillations to rest. For $p = 0.001$, $f = 0.3$ we find $\delta_H = 0.191$, $\delta_1 = 0.197$, $\delta_2 = 0.205$, $\delta_L = 0.269$.

It is clear through the analogy with scalar bistable reaction–diffusion equations why there should be transition fronts in the form of traveling waves in the present models. What is surprising and perhaps counter-intuitive is why localized regions of oscillation should exist in these models. The phenomenon is dependent on the dispersive properties of the medium, for example, the parameter q in the $\lambda - \omega$ model. Suppose that a region of medium at rest is excited past threshold. Then the dynamics push it toward the limit cycle and diffusion propagates this excitation. However, the strong dispersive properties of the waves tend to cause the waves to have a high wave number k. In the $\lambda - \omega$ systems this counteracts the excitation of diffusion. The diffusive and dispersive "forces" balance and one is left with a region that cannot propagate but also which cannot collapse back to rest.

3.2. Stability and existence of the localized oscillation

In a finite domain with Neumann boundary conditions, we can pose the existence of the localized oscillation for the $\lambda - \omega$ model as a boundary value problem and solve it numerically. We are interested in solutions of the form

$$u(x,t) + iv(x,t) = r(x)e^{i\Omega t + \int_0^x \phi(y)\,dy}, \tag{3.1}$$

which satisfy, $(r', \phi) = (0, 0)$ at the boundaries, $x = 0$, $x = L$. We require that $r(x)$ be monotone decreasing so that it has a maximum at $x = 0$. This corresponds to a localized oscillation at the left end of the medium. We numerically solve this boundary value problem using a version of the program AUTO. Fig. 8(A) shows the amplitude of $r(0)$ as a function of the threshold a for $q = 0.4$. It is evident from the picture that there are intervals of a where there are at least two different peaks and for a large enough, there are no solutions of the desired form. This type of calculation gives no insight into the stability of the localized oscillator and how stability is lost. Thus, we will briefly look at the discrete analog of the model. This allows us to study the existence and stability of the localized oscillation as a dynamical system. We fix $q > 0$ and choose a so that there is a localized oscillatory region. We then vary a and study this bifurcation picture. We discretize the $\lambda - \omega$ system into 20 compartments. The coupling between compartments is $d = 1$ and we set $q = 0.4$. We start with $a = 0.2$ and find that there is the discrete analog of the localized oscillation. That is the amplitude, $R_j = \sqrt{u_j^2 + v_j^2}$ is constant over time and decreases with j. Fig. 8(B) plots the amplitude R_1 as a function of the parameter a. The diagram for the discrete system is similar to that of the continuous one; both have a turning point where the solution with amplitude close to 1 meets a smaller amplitude solution. In the spatially discrete model, the lower branch of solutions appears to always be unstable. The upper branch is stable for a large enough and then loses stability at a torus bifurcation. The brief results here suggest that the localized oscillations are lost at a saddle-node bifurcation for limit cycles for increasing threshold and at a torus bifurcation for decreasing threshold.

3.3. Interaction of the oscillators

We have numerically shown that there are spatially localized oscillations in the bistable medium for a certain range of parameters. One natural question is whether there can be several localized regions that oscillate? and if so, how do they interact with one another. This is easiest to answer numerically. Fig. 9 shows two examples of solutions to (2.3) with localized spatial disturbances of the stable rest state. In Fig. 9(A), the two pulses are close to each

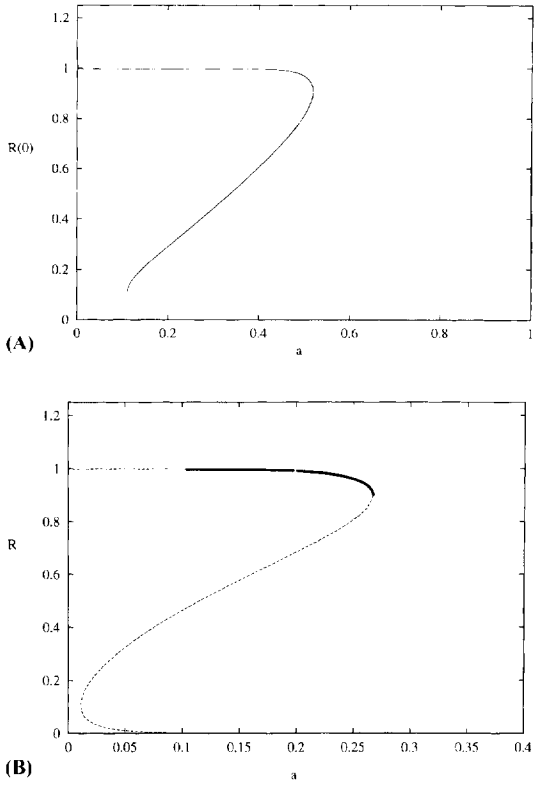

Fig. 8. Structure of the pulse solution as a function of the threshold parameter a for $q = 0.4$ in the $\lambda - \omega$ model. (A) The magnitude at $x = 0$ of the oscillation for the continuous boundary value problem on the interval $[0, 1]$. (B) The analogous calculation for the discretized model. This shows the stability of the solution; solid lines are stable and dashed are unstable.

other and they merge into a single pulse which then persists. If they are started far enough apart, then they remain intact and "push" each other to their respective boundaries where they remain. They quicky achieve a stationary amplitude but the phases continue to interact. Eventually, they settle into a state in which the oscillation at $x = 0$ is 180° out of phase with the oscillation at the other end.

A similar behavior occurs for the $\lambda - \omega$ system; eventually, the local oscillations migrate to the boundaries and establish an anti-phase relationship. Fig. 10(A) shows the amplitude $r = \sqrt{u^2 + v^2}$ and the phase gradient $\phi = \theta_x$. Fig. 10(B) shows the relative phase $\theta(x, t) - \theta(0, t)$. There are several interesting features. The amplitude is continuous but not differentiable at the point in the center of the medium $x = \frac{1}{2}L$. The amplitude vanishes at $x = \frac{1}{2}L$ and the relative phase undergoes a jump of π at this point. The phase gradient is continuous (except at $x = \frac{1}{2}L$) and anti-symmetric across the center of the medium. For comparison, the relative phase of the (unstable) synchronous double pulse solution is also shown. (In the synchronous double pulse solution, the amplitude is differentiable at $x = \frac{1}{2}L$ and the derivative vanishes while the amplitude itself remains positive.) As with the single pulse, the existence of the double pulse can be posed as a third-order boundary value problem. The solution is as in

Fig. 9. Evolution of two localized disturbances for the chemical model. (A) Two close-by perturbations merge and form a single local spatial oscillator at the left edge. Parameters as in Fig. 7 except total simulation time is 250. (B) Two perturbations farther apart push each other to the edges and eventually settle into an *antiphase* oscillatory state. Parameters as in Fig. 7.

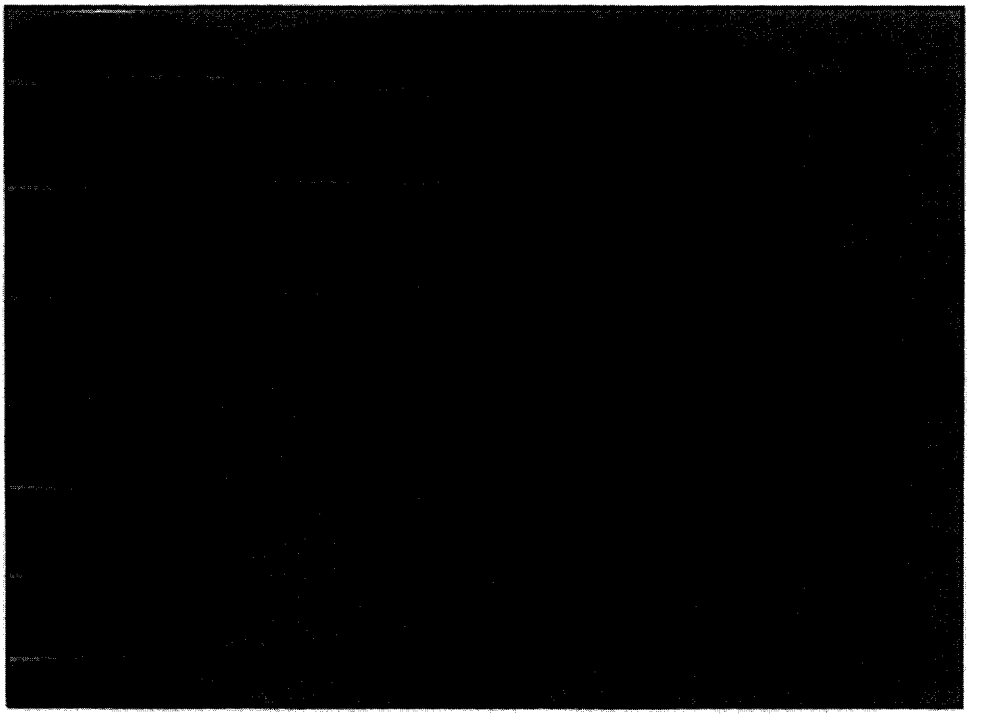

(A)

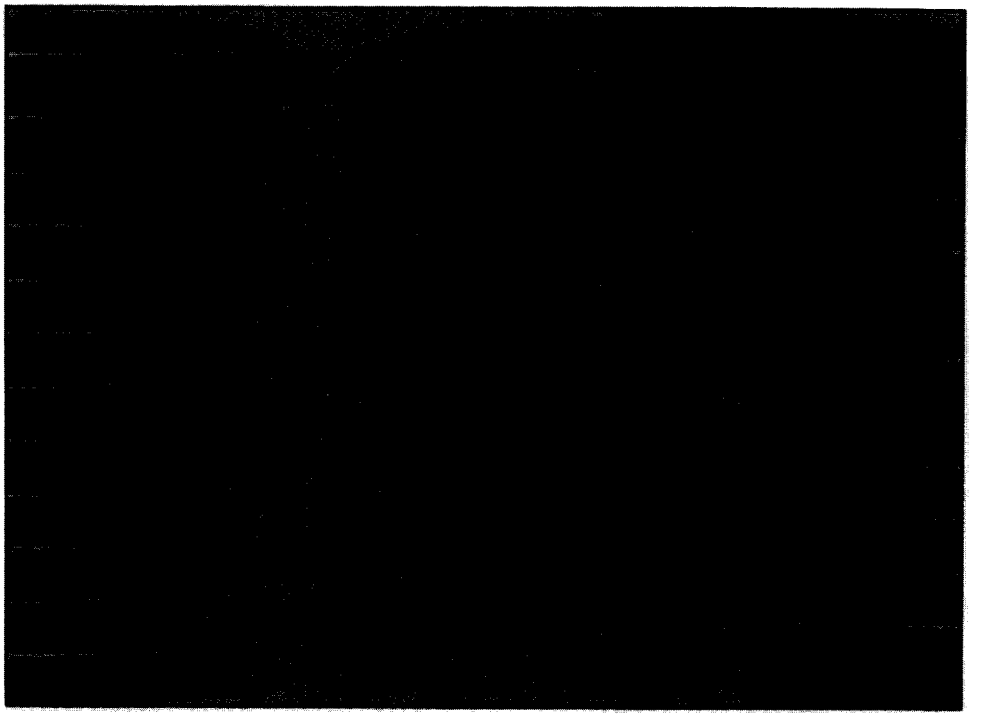

(B)

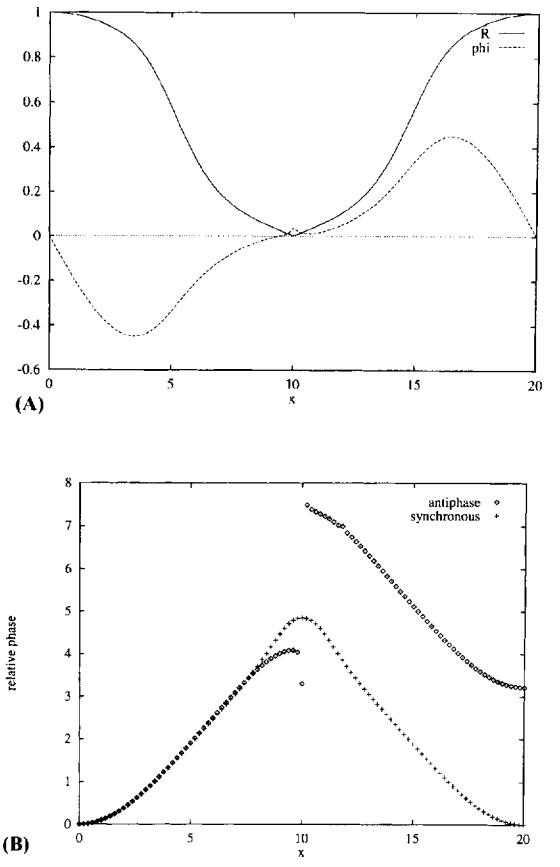

Fig. 10. Double pulse behavior of the $\lambda - \omega$ system. (A) The steady state magnitude, R and the steady state phase-gradient ϕ as functions of spatial position. Both the synchronous and the anti-phase solutions have the same profiles. Parameters as in Fig. 6. (B) The relative phase of the solutions for initial data that are synchronous or anti-phase as a function of spatial position. Note that the profiles are quite similar but the anti-phase solution has a jump of π at $x = 10$.

(3.1) but with the following boundary conditions:

$$r'(0) = 0, \quad \phi(0) = 0, \quad r(\tfrac{1}{2}L) = 0, \quad \phi(\tfrac{1}{2}L) = 0.$$

In two dimensions, solitary and multiple regions of oscillatory activity also occur and interact in much the same ways as on the line. Thus, this phenomena should be observable in real chemical media if the parameters are chosen correctly. Essentially, the pattern of a single localized region looks like a "target pattern" which fails to propagate. As in one dimension, two nearby disturbances will be absorbed into a single region. Unlike the interactions of target patterns, where the "fastest" one eventually takes over the medium, the present patterns damp out quickly enough that the interactions generally result only in perturbations of the phase. We have not been able to detect any movement of these solitary pulses other than merging of closeby regions but that may be due to the discretization of the medium. ("Movies" of the two-dimensional simulations can be found at the URL: `ftp://mthbard.math.pitt.edu/pub/bardware/movies/movie.html`.) With multiple localized oscillators, they often organize themselves into a fixed pattern of phases much like weakly coupled oscillators. In other cases the phases between the localized pulses drift and they appear uncoupled.

Haim et al. [5] observe target like patterns in a flow reactor but the mechanism seems quite different from the present case. Kobayashi et al. [9] numerically simulated two-dimensional patterns in the parameter regime where there are wave fronts and found the analog of target and spiral waves. They did not consider the parameter regime where there are localized oscillations.

4. Discussion

We have shown that a medium that has both a stable fixed point and a stable limit cycle separated (in phase space) by an unstable orbit is capable of producing a traveling wave front that joins these two states. Like a reaction–diffusion system with two stable fixed points, the direction of the front propagation depends on the position of the separatrix. Unlike the medium with two stable *fixed points* there is a regime of parameters where the medium can support many localized regions of oscillatory activity separated by regions of quiescence. These localized regions become analogous to coupled pacemakers whose activity fails to propagate but interact weakly through the quiescent regions in between. The wavefronts are quite different from those found by Sherratt [13,14] in that their velocity is independent of initial data and they appear to be unique.

We have explicitly solved the wavefront dynamics for a $\lambda - \omega$ system but the existence of these waves for general reaction–diffusion equations remains an open mathematical problem. Simulations seem to indicate that these solutions do exist. The transition from waves to the localized oscillatory patches appears to be complicated and has not been answered in this paper. The existence of a single localized oscillatory patch in a finite domain with noflux boundary conditions also remains an open problem although for the $\lambda - \omega$ systems, it is just a three-dimensional shooting problem (see Eq. (3.1)). Numerical simulations indicate that localized oscillations that are slightly off center eventually move to the boundaries of the medium. However, this migration can be extremely slow and from an experimental point of view may be negligible.

There are other mechanisms that can lead to coexistence of a stable limit cycle and a stable fixed point. Fig. 11 shows one such mechanism. For a range of the parameter α there coexists three fixed points and a limit cycle. Only the lower fixed point is stable; the middle point is a saddle point and the third fixed point is an unstable node. The stable manifold of the saddle point separates the basin of attraction of the limit cycle and the stable fixed point. This mechanism is seen in chemical systems [2] and some nerve models [6]. As in the bistable studied here, there are parameter regimes in which there are fronts that switch the medium from the stable fixed point and the front velocity appears to be unique. However, the resulting wave leaves a chaotic wake much like that observed by Sherratt [15].

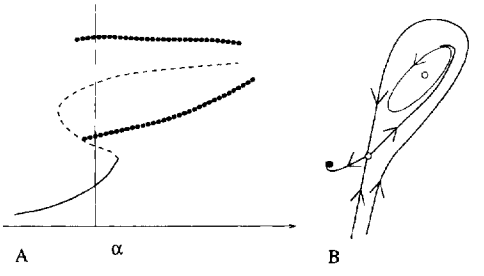

Fig. 11. Another mechanism for bistability involving a saddle-point separatrix. (A) Schematic bifurcation diagram with parameter α. Upper branch is an unstable node, middle branch is a saddle-point, and lower branch is stable. The upper fixed point is surrounded by a stable periodic solution which is lost at a homoclinic bifurcation when it contacts the middle branch. (B) Phase plane corresponding to the value of α indicated in A. The two branches of the stable manifold for the saddle point separate the basins of attraction of the limit cycle and the fixed point.

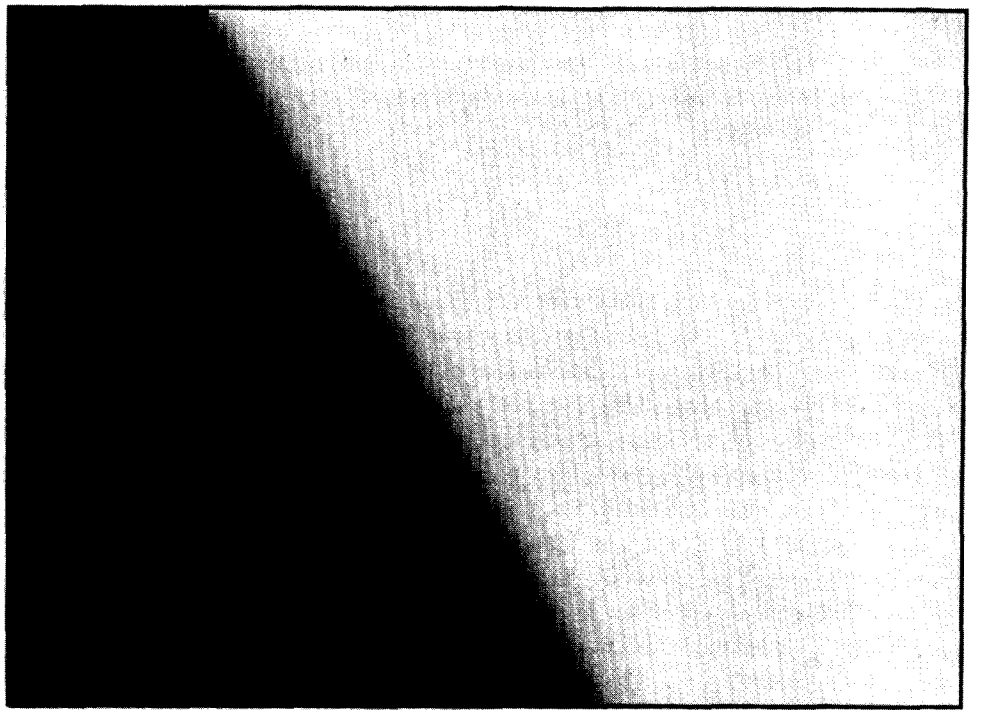

Fig. 12. Switching front for the Hindmarsh–Rose equations, $v_t = w - v^3 + 3v^2 + 0.15 + 0.2v_{xx}$, $w_t = 1 - 5v^2 - w + 0.2w_{xx}$, on the interval $0 < x < 20$ for total time of 150. Amplitude of w is shown by grey scales (white is $w = -10$ and black is $w = 1.$). The front velocity is very regular but the behavior in back of the front is chaotic.

Fig. 12 shows a simulation of the fast dynamics of the Hindmarsh–Rose model in the bistable regime. Although the synchronous oscillatory solution is a stable solution for this particular set of parameters (and, therefore, there will be a family of stable wavetrains with long wavelengths), the wave front apparently induces too much of a phase gradient and the short waves that would be required to support this gradient are unstable. The existence of wavefronts for this model remains an open question.

We have shown that there are switching fronts from rest to an oscillatory state in systems of bistable reaction diffusion systems that exhibit subcritical Hopf bifurcations. In certain parameter ranges there exits the possibility of local oscillatory patches. Since reaction kinetics with subcritical Hopf bifurcations are fairly common, it should possible to observe the spatially localized oscillations in an experimental situation in one- and two-dimensions.

References

[1] M.C. Cross and P.C. Hohenberg, Pattern formation outside of equilibrium, Rev. Mod. Phys. (1993) 851–1112.
[2] A.K. Dutt and S.C. Muller, Bistability in an uncatalyzed bromate oscillator in a continuously stirred tank reactor, J. Chem. Phys. 104 (1996) 583–586.
[3] R.J. Field and M. Burger, eds., Oscillations and Traveling Waves in Chemical Systems (Wiley, New York, 1985).
[4] P.C. Fife and J.B. McLeod, The approach of solutions of nonlinear diffusion equations to travelling front solutions, Arch. Rat. Mech. Anal. 65 (1977) 335–361.
[5] D. Haim, G. Li, Q. Ouyang, W.D. McCormick, H.L. Swinney, A. Hagberg and E. Meron, Breathing spots in a reaction–diffusion system, preprint (1996).
[6] J.L. Hindmarsh and R.M. Rose, A model of neuronal bursting using three coupled first order differential equations, Proc. Roy. Soc. London B 221 (1984) 87–102.

[7] R. Kapral and K. Showalter, eds., Chemical waves and Patterns (Kluwer, Dordrecht, 1995).
[8] G.A. Klassen and W.C. Troy, The stability of travelling wave front solutions of a reaction–diffusion system, SIAM J. Appl. Math. 36 (1981) 89–98.
[9] R. Kobayashi, T. Ohta and Y. Hayase, Self-organized pulse generator, Physica D 84 (1995) 162–170.
[10] N. Kopell and L.N. Howard, Plane wave solutions to reaction–diffusion equations, Stud. Appl. Math. 52 (1973) 291–328.
[11] J.D. Murray, Mathematical Biology (Springer, New York, 1993).
[12] J.E. Pearson, Complex patterns in a simple system, Science 261 (1993) 189–192.
[13] J.A. Sherratt, The amplitude of periodic plane-waves depends on initial conditions in a variety of $\lambda - \omega$ systems, Nonlinearity 6 (1993) 1055–1066.
[14] J.A. Sherratt, On the evolution of periodic plane-waves in reaction–diffusion systems of $\lambda - \omega$ type, SIAM J. Appl. Math. 54 (1994) 13.
[15] J.A. Sherratt, Unstable wavetrains and chaotic wakes in reaction–diffusion systems of $\lambda - \omega$ type, Physica D 82 (1995) 165–179.
[16] O. Thual and S. Fauve, Localized structures generated by subcritical instabilities, J. Phys. (Paris) 49 (1988) 1829–1833.
[17] P.C. Fife, 1978.